

Provided for non-commercial research and education use.  
Not for reproduction, distribution or commercial use.



This article appeared in a journal published by Elsevier. The attached copy is furnished to the author for internal non-commercial research and education use, including for instruction at the authors institution and sharing with colleagues.

Other uses, including reproduction and distribution, or selling or licensing copies, or posting to personal, institutional or third party websites are prohibited.

In most cases authors are permitted to post their version of the article (e.g. in Word or Tex form) to their personal website or institutional repository. Authors requiring further information regarding Elsevier's archiving and manuscript policies are encouraged to visit:

<http://www.elsevier.com/copyright>



# Experiments and validation of a model for microparticle detachment from a surface by turbulent air flow

A.H. Ibrahim, P.F. Dunn\*, M.F. Qazi

*107 Hessert Laboratory, Notre Dame, IN 46556, USA*

Received 23 October 2006; received in revised form 26 March 2008; accepted 26 March 2008

---

## Abstract

This work presents a revised model for microparticle detachment from a surface by turbulent air flow. The model accounts for the dependence of the effective surface roughness at the microparticle/surface interface on the contact radius. This dependence is quantified by surface scanning using atomic force microscopy. A series of detachment experiments of glass microparticles, ranging from 30 to 110  $\mu\text{m}$  in diameter, from a glass substrate, was conducted to validate the revised model. The model and data were found to agree at the 95% confidence level. The model sensitivity to five different physical factors was analyzed using design-of-experiments methodology with a full-factorial-design layout. The uncertainty in the threshold-detachment free-stream velocity that arose from the inherent variability in the model inputs was quantified using Monte Carlo simulations. The uncertainty that occurs in the threshold-detachment free-stream velocity when there is no specific information on surface roughness was estimated.

© 2008 Elsevier Ltd. All rights reserved.

*Keywords:* Microparticle; Detachment; Pull-off; Adhesion; AFM; Roughness; Asperity height; Sensitivity; Design of experiments; Monte Carlo

---

## 1. Introduction

The detachment of particles from surfaces and their subsequent entrainment into air flow occur in many natural and industrial applications. Two environmentally related examples include particle filtration and the dispersion of microparticle pollutants from surfaces into the atmosphere. Previous studies in this area have provided different models and data for the detachment process and have identified the major factors governing this process. Among these factors are those affecting the particle's adhesion force and moment and those affecting its removing forces and moments. Those affecting the particle's adhesion force and moment include the particle size, the particle and surface material properties, the air relative humidity (for example, Podczeczek, Newton, & James, 1997; Quon, Ulman, & Vanderlick, 2000), the standard deviation of the surface asperity heights (Cheng, Brach, & Dunn, 2002), the residence time between that of surface deposition and flow application (for example, Ibrahim, Dunn, & Brach, 2003b), and the measurement technique used to assess particle adhesion to the surface (Mollinger, 1995). Those affecting the particle removing forces and moments include the particle size, the type of flow (laminar or turbulent) (Ibrahim et al., 2003b), the presence and the intensity of turbulent burst-sweep events (Soltani & Ahmadi, 1995), and the temporal mean flow acceleration (Ibrahim & Dunn, 2006). Ziskind (2006), Ziskind, Fichman, and Gutfinger (1995), Nicholson (1988), and Sehmel (1980) have

---

\* Corresponding author.

*E-mail address:* [pdunn@nd.edu](mailto:pdunn@nd.edu) (P.F. Dunn).

provided extensive reviews on the subject. Additional references cited by the authors in a series of detachment-related studies can be found in Ibrahim, Dunn, and Brach (2003a, 2003b, 2004), Ibrahim (2004), Ibrahim and Dunn (2006) and Cheng et al. (2002).

The flow velocities that induce the detachment of glass microparticles from glass surfaces have been measured by different investigators. Zimon (1982) reported velocities ranging from 8 to 10 m/s that were required to detach glass microparticles of 21  $\mu\text{m}$  in diameter; Taheri and Bragg (1992) measured equivalent free-stream velocities of 28 and 22 m/s that were necessary to detach 50% of glass particles of 20 and 35  $\mu\text{m}$ , respectively. This relatively large range of the reported detachment velocities for the same types of particles and surfaces most likely was the result of variations in surface roughness and air relative humidity within and between these studies. Detachment is quite sensitive to these and other variables. Their control and measurement during experiments are critical to obtaining reproducible data that can be used to validate models of this process.

The objectives of the current work are several. The first is to provide a systematic study of microparticle detachment for several microparticle diameters under well-controlled conditions (to the authors' knowledge, experimental results under controlled conditions of this extent have not appeared in the literature). The second is to present a revised microparticle detachment model that describes these data to within 95% confidence. The third is to provide an estimate of the model's uncertainty, the fourth is to estimate the uncertainty that arises when no specific information on the surface roughness is available, and the fifth is to examine the sensitivity of the model to the different physical factors that govern the detachment process.

In this paper, the term *detachment* refers to the process of breaking the adhesion bond between the microparticle and the surface. Detachment can be observed experimentally. It occurs when the microparticle initially begins to move on the surface. The term *rough-surface pull-off force* refers to the actual force required to break the adhesion bond between the microparticle and the surface. This force is smaller than the smooth-surface pull-off force, which occurs in the case of a perfectly smooth interface. The ratio of the rough-to-smooth surface pull-off forces (hereafter referred to as  $C$ ) can be estimated using the theoretical results of Cheng et al. (2002) coupled with measurements of the surface asperity heights obtained using an atomic force microscope (AFM). Further, microparticle detachment from a surface is characterized by the detachment fraction versus the free-stream velocity. This fraction is defined as  $n^*(t) = 1 - [n(t)/n(0)]$ , in which  $n(t)$  is the number of non-detached microparticles on the surface at time  $t$ . The 50% threshold-detachment free-stream velocity,  $U_{\text{th},50\%}$ , is defined as the free-stream velocity at which the detachment fraction equals 0.50.

## 2. Experimental configuration

Details of the experimental facility and diagnostics used for this study have been described previously (Ibrahim et al., 2003a, 2003b). Only the features related directly to this study are presented here. A schematic of the experimental facility is shown in Fig. 1. For all experiments, the tunnel's programmable controller was set to achieve a mean temporal-flow acceleration of approximately  $0.13 \text{ m/s}^2$  in the transient-flow phase and final free-stream flow velocities of either 5, 8, 15, or 24 m/s. The air temperature and relative humidity were  $22^\circ\text{C} \pm 1^\circ\text{C}$  and  $29\% \pm 3\%$ , respectively, during all experiments.

Detachment situations can be characterized in terms of either a free-stream velocity,  $U_\infty$ , or a friction velocity,  $u^*$ , defined as  $\sqrt{\tau_w/\rho}$ , where  $\tau_w$  is the wall shear stress and  $\rho$  is the density of the flowing medium. In this work, the free-stream and friction velocities (in units of m/s) were correlated by the least-squares linear-regression expression  $u^* = 0.0375U_\infty + 0.0387$  with an uncertainty of  $\pm 0.0300$  at a 95% confidence level (Ibrahim et al., 2003a).

The free-stream velocity was measured using a Pitot-static tube and an inclined manometer. Microvideophotographic images were acquired simultaneously in the top view. The images were made with a Basler A501K progressive-scan CMOS monochromatic digital camera and magnifying lenses (Micro Nikkor 105 mm lens and 2X/4X Nikon teleconverters) in order to achieve enough optical magnification to resolve individual microsphere motion. The camera had a resolution of 1280 pixels  $\times$  1024 pixels and was operated at 30 frames per second and a shutter speed approximately equal to the inverse of the frame rate. The number of microparticles on the surface at a given free-stream velocity was determined from the images through manual count.

The actual microparticle diameters for the experiments performed were  $30.1 \mu\text{m} \pm 2.1 \mu\text{m}$ ,  $52.6 \mu\text{m} \pm 3.2 \mu\text{m}$ ,  $72.6 \mu\text{m} \pm 4.4 \mu\text{m}$ ,  $90.3 \mu\text{m} \pm 4.5 \mu\text{m}$ , and  $111 \mu\text{m} \pm 5.5 \mu\text{m}$ . All microparticles were soda lime glass obtained from Duke Scientific Corporation, catalogue numbers 9030, 9050, 9070, 9090, and 9110, respectively. The microparticle

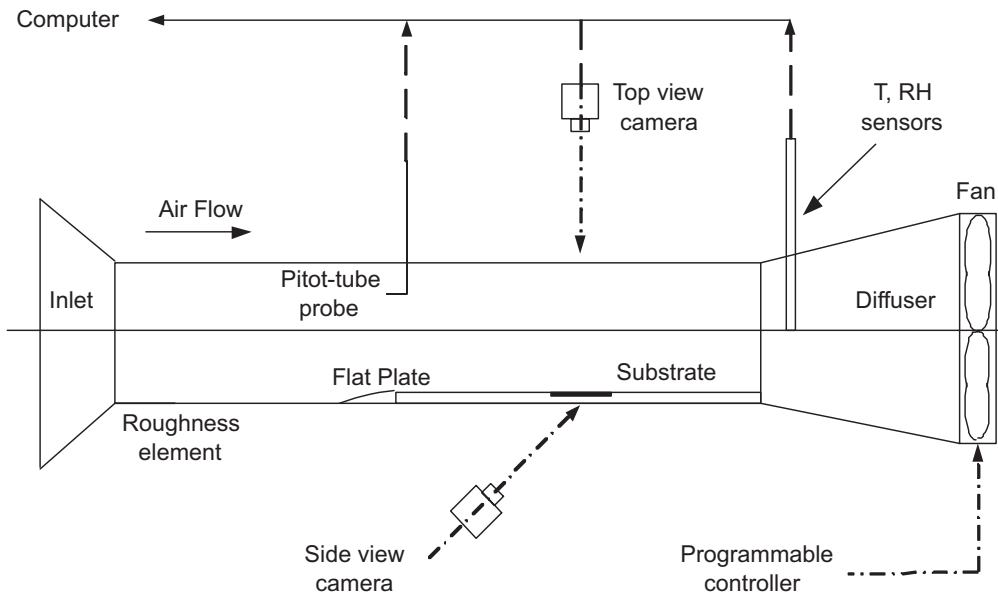


Fig. 1. Schematic of the experimental facility.

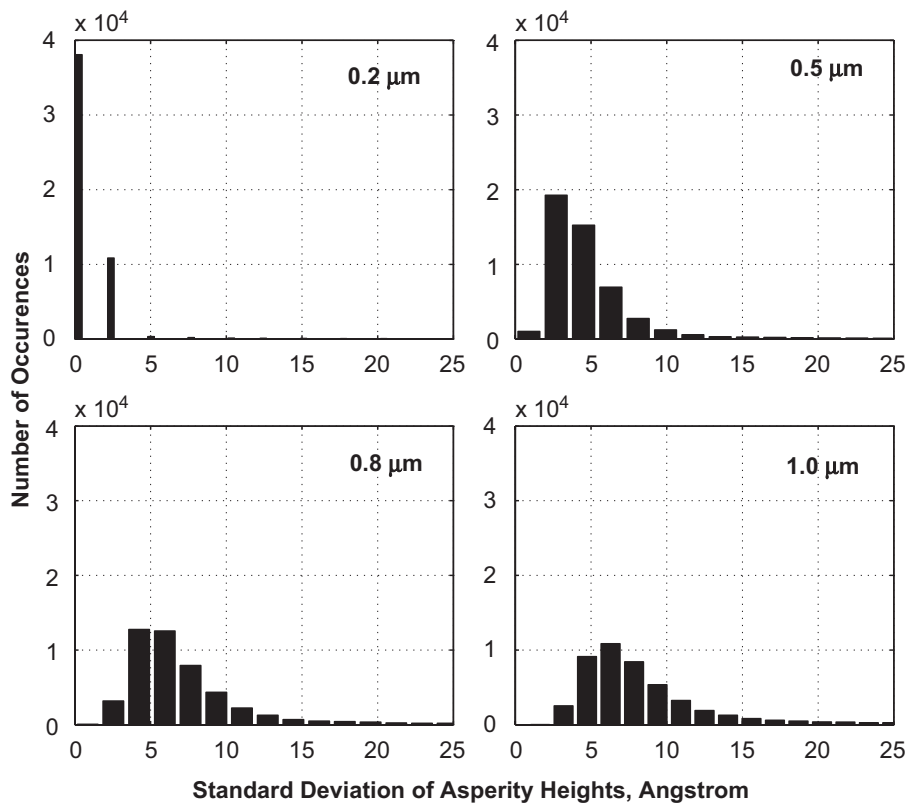


Fig. 2. Histograms of the standard deviation of heights for four different contact radii ranging from 0.2 to 1  $\mu\text{m}$ .

density was approximately  $2400 \text{ kg/m}^3$ . For each of the diameters, the experiment was repeated five times under the same conditions to estimate the uncertainty of repeatability. The microparticles were always embedded completely within the viscous sublayer of the boundary layer for the size range and flow velocities considered. The microparticles were deposited as a sparse monolayer ( $< \sim 50 \text{ microparticles/cm}^2$ ) on the glass substrate. Deposition was made

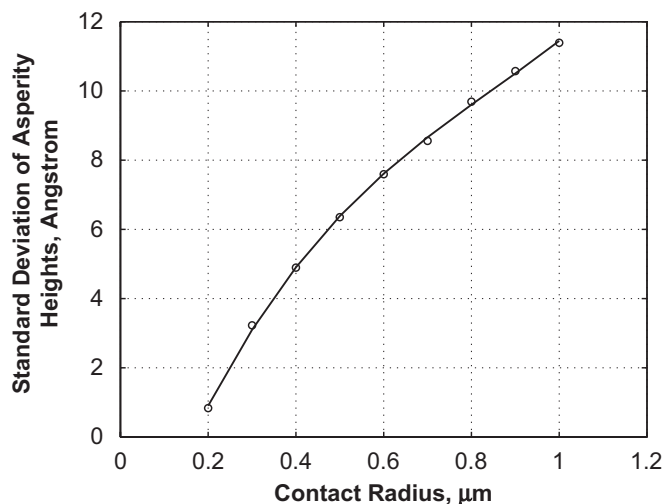


Fig. 3. Variation of the standard deviation of asperity heights versus the contact radius. Calculated values from measurements are shown as open circles and the best-fit polynomial as a solid curve.

by gravitational settling from approximately 10 cm above the surface immediately before initiation of the flow. Any agglomerates or microparticles removed by collisions were excluded from the detachment count.

Similar glass substrates were used (Amersham Pharmacia; 10 cm  $\times$  10.5 cm  $\times$  1.27 mm). The substrates were prepared prior to each experiment by cleaning it with phosphate-free detergent, immersing it in dilute nitric acid (1:1) for 60 s, rinsing it in distilled water for 120 s, and then heating it at 200 °C for 1 h. All substrates were kept in a dry, warm enclosure until used. This surface preparation technique was similar to that given by Phares, Smedley, and Flagan (2000).

The surface-roughness profile of one of the substrates was measured using an AFM. The scan area was 100  $\mu\text{m}$   $\times$  100  $\mu\text{m}$  with a resolution of 5 pixels/ $\mu\text{m}$ . The standard deviation of asperity heights was estimated for square areas of lengths ranging from 0.2 to 1.0  $\mu\text{m}$ . For each radius, 50 000 estimates were made for different squares in random positions within the 100  $\mu\text{m}$   $\times$  100  $\mu\text{m}$  scan area.

The histograms of four selected radii are shown in Fig. 2. As the square scan area increases, the range of the standard deviation of the surface asperity heights also increases. The means of the measured standard deviations are plotted in Fig. 3 versus their equivalent circular contact radii. As the contact radius,  $a$ , decreases, the mean of the standard deviation of asperity heights,  $\sigma$ , decreases, effectively giving rise to a smoother surface. This is because a microparticle is affected by a smaller range of asperity roughness as its contact radius is decreased.

These considerations imply that microparticles of different radii have different surface roughness profiles, and, therefore, according to Cheng et al. (2002), have different rough-surface pull-off forces and different values of  $C$ . This is in contrast to the detachment model presented in Ibrahim et al. (2003a) that assumed a constant standard deviation of asperity height and, therefore, a constant value of  $C$  for all microparticle sizes. For the specific surface and range of contact radii investigated in this study, the relationship between  $\sigma$ , in  $\text{\AA}$ , versus  $a$ , in  $\mu\text{m}$ , can be fitted with a third-order polynomial, which is shown as a solid curve in the figure. The resulting expression is  $\sigma = 3.07a^3 - 13.62a^2 + 25.47a - 3.48$ .

### 3. Experimental results

The results of the detachment experiments are shown in Fig. 4. In this figure, the progress of the detachment fraction versus the free-stream velocity for each of the five diameters studied is shown. It can be seen that larger microparticles detach at smaller flow velocities. The 'no-slip' velocity condition at the surface makes it increasingly difficult to provide sufficient removing forces or moments as the microparticle size gets smaller. Also, all curves exhibit a sigmoid shape, which is typical of the relationship between the detachment fraction,  $n^*$ , and the free-stream velocity,  $U_\infty$ . The experimental  $U_{\text{th},50\%}$  values and their precision uncertainty estimates are shown in Fig. 5. Also presented in the figure are the theoretical predictions of the model that will be considered next.

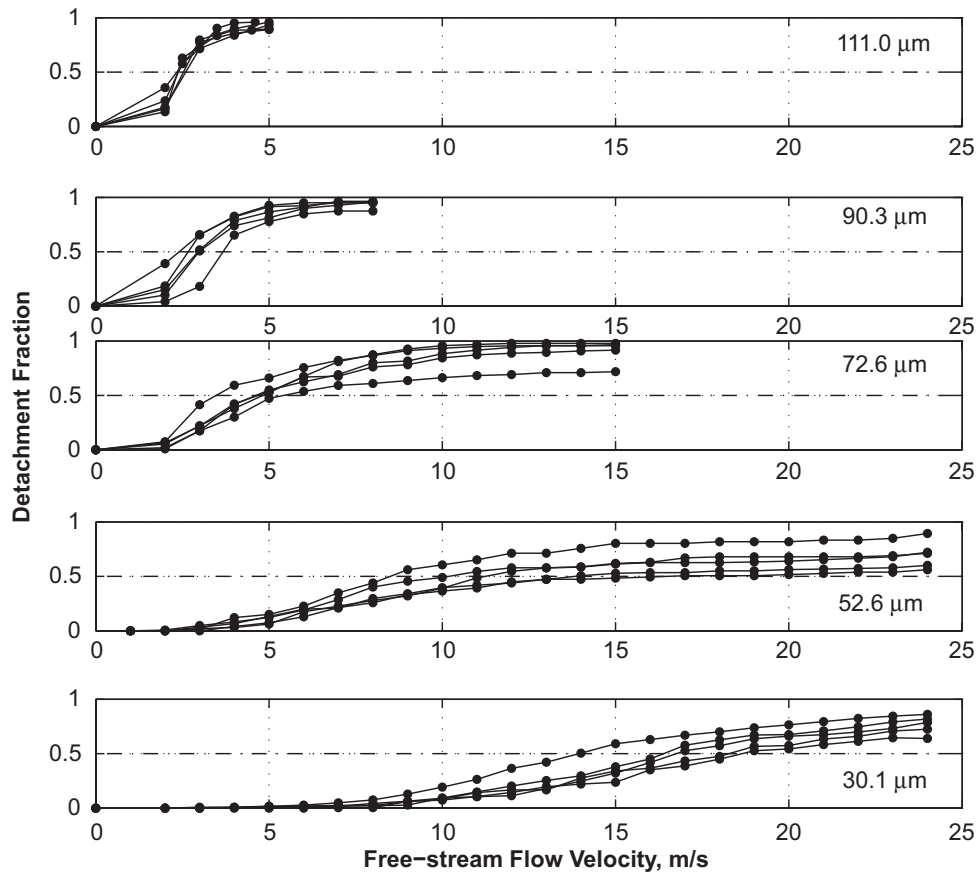


Fig. 4. The progress of the detachment fraction versus the free-stream velocity for all the cases considered. Five repeated experiments were conducted for each of the five diameter cases examined.

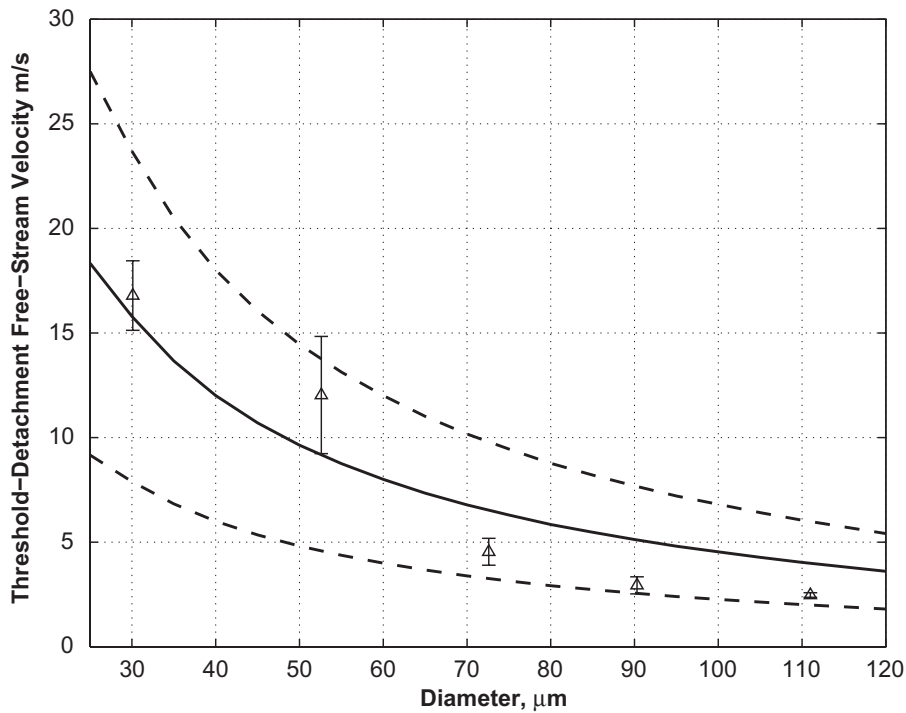


Fig. 5. The threshold-detachment free-stream velocity versus microparticle diameter. The solid curve is the theoretical prediction of  $U_{th,50\%}$  with a variable  $C$  (current model). The dotted curves are the 95% confidence limits of the variable- $C$  model determined from the Monte Carlo analysis. The symbols denote the average measured  $U_{th,50\%}$  along with their precision uncertainties.

#### 4. Detachment model

Force and moment-balance detachment models for individual microspheres on a surface embedded in a viscous sublayer have been proposed by Cleaver and Yates (1973), Braaten, Paw, and Shaw (1990), Tsai, Pui, and Liu (1991), Cabrejos and Klinzing (1992), Soltani and Ahmadi (1994), Yiantsios and Karabelas (1995), Ziskind, Fichman, and Gutfinger (1997), Hontanon, de los Reyes, and Capitaio (2000) and Ibrahim et al. (2003a). The current model is a revised form of the model presented by Ibrahim et al. (2003a). The main difference between this and previous models is that the revised model accounts for the dependence of the effective surface roughness on the contact radius.

A schematic of a microparticle attached to a surface and the forces acting on it at the moment of detachment is presented in Fig. 6. Five forces are shown: the mean aerodynamic lift force,  $F_L$ , in the upward vertical direction, the gravitational force,  $F_G (=mg)$ , and the rough-surface pull-off force,  $F_{PO}$ , both in the downward vertical direction, the mean aerodynamic drag force,  $F_D$ , in the forward horizontal direction and the friction force,  $F_F$ , in the reverse horizontal direction.

The microparticles used in these experiments resided fully in the viscous sublayer, which is defined by wall-unit height  $y^+ < 5$ . The wall unit  $y^+$  equals  $yu^*/\nu$  in which  $y$  is the physical height above the wall and  $\nu$  is the dynamic viscosity of the flowing medium. The velocities  $u$  and  $w$  are the stream-wise and the normal-mean flow velocities, respectively. In the viscous sublayer, the flow is usually described by the normalized velocities  $u^+$  and  $w^+$ , where  $u^+ = u/u^*$  and  $w^+ = w/u^*$ . It has been observed that the detachment of microparticles from the viscous sublayer is associated with specific flow structures inside the viscous sublayer known as the burst-sweep events (for example, Braaten, Shaw, & Paw, 1993). These events have higher flow velocities in the stream-wise and normal-flow directions and are described by Eqs. (9)–(11), which are presented later.

Three detachment modes are possible, namely direct lift-off, where

$$F_L > F_{PO} + mg, \tag{1}$$

and sliding, where

$$F_D > k_s(F_{PO} + mg - F_L), \tag{2}$$

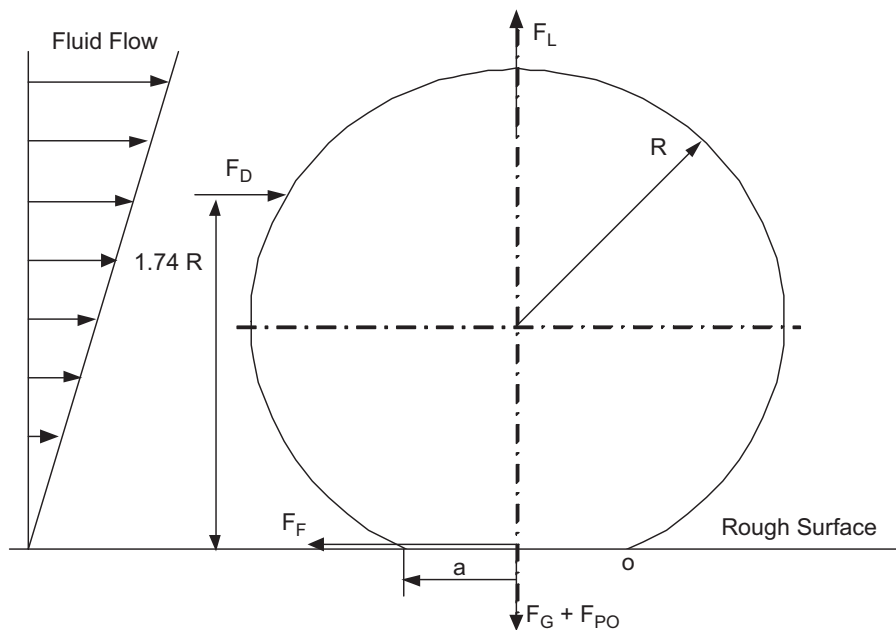


Fig. 6. A schematic of a microparticle attached to a surface and the forces acting on it at the moment of detachment.

in which  $k_s$  is the static coefficient of friction, and, rolling, where

$$1.74RF_D + aF_L > a(F_{PO} + mg), \quad (3)$$

in which  $R$  is the microparticle diameter and  $a$  is the microparticle contact radius, as determined using Eq. (6).

The values of these forces and moments show that among the three possible detachment mechanisms, rolling provides the least resistance for incipient detachment, as compared to sliding or direct lift-off. Throughout the remainder of this work, rolling is considered as the mechanism of initial detachment, as specified by Eq. (3).

The smooth-surface pull-off force,  $F_{PO,s}$ , was estimated from the results of Johnson and Greenwood (1997), in which the Leonard-Jones potential was used to calculate the pull-off force at the DMT-JKR transition (Derjaguin, Muller, & Toporov, 1975; Johnson, Kendall, & Roberts, 1971). According to these calculations, the smooth-surface pull-off force is  $1.57\pi\gamma R$  and  $1.58\pi\gamma R$  for 110  $\mu\text{m}$  diameter glass and 30  $\mu\text{m}$  diameter glass microspheres, respectively.

The rough-surface pull-off force is estimated as

$$F_{PO} = C F_{PO,s}, \quad (4)$$

in which the factor  $C$  is a function of the standard deviation of the asperity heights,  $\sigma$ . The value of  $\sigma$  is obtained from

$$\sigma = \sqrt{\sigma_s + \sigma_p}, \quad (5)$$

in which  $\sigma_s$  is the standard deviation of asperity heights of the surface for a given microparticle contact radius and  $\sigma_p$  is the standard deviation of asperity heights of the microparticle in the interface region. In this study,  $\sigma_p$  was assumed to be equal to  $\sigma_s$ .

The contact radius,  $a$ , is evaluated using JKR theory, where

$$a = \frac{6\pi\gamma R^2}{K}, \quad (6)$$

in which  $\gamma$  is the surface energy of adhesion.  $K$  is the composite Young's modulus given by

$$K = \frac{4}{3} \left[ \frac{1 - \nu_1^2}{E_1} + \frac{1 - \nu_2^2}{E_2} \right]^{-1}, \quad (7)$$

in which  $E_1$  and  $E_2$  are the values of Young's modulus and  $\nu_1$  and  $\nu_2$  are the values of Poisson's ratio for the microparticle and the surface, respectively.

The aerodynamic drag force was modelled as Stokesian drag, equal to  $3\pi\mu d u_c$ , with corrections made for inertial (Ockendon & Evans, 1972) and wall effects (O'Neill, 1968). The velocity  $u_c$  is the flow velocity at a height from the wall equal to the microparticle radius, or  $d/2$ . Slip correction (Friedlander, 1977) was neglected because of the relatively large microparticle diameters used in this study. The shear effect on drag also is weak and can be neglected (Kurose & Komori, 1999). The buoyancy, virtual mass, and Basset forces are much less than the drag force because the density of the microspheres in the present experiments ( $2470 \text{ kg/m}^3$ ) is much larger than that of air. The mean aerodynamic drag force consequently is modelled as

$$F_D = 3f\pi\mu d u_c [1 + 3Re_P/8 + 9Re_P^2 \ln(Re_P)/40 + 0.1879Re_P^2]. \quad (8)$$

The factor  $f$  ( $=1.7009$ ) accounts for the wall effect. The microparticle Reynolds number,  $Re_P$ , is defined as  $u_c R/\nu$ . In this work, the maximum  $Re_P$  was approximately 4.

Inside the viscous sublayer, burst-sweep events occur and cause an instantaneous increase in flow velocities, which facilitates the detachment process. Soltani and Ahmadi (1994) proposed a sublayer model for the turbulent burst-sweep event. According to this model

$$u^+ = 1.74y^+ + 0.1y^{+2} \quad (9)$$

and

$$w^+ = 0.54u^+. \quad (10)$$

Soltani and Ahmadi (1995) performed a direct numerical simulation of microparticle entrainment in a turbulent channel flow and described the variation in the intensity of these events. Their results show that during a burst-sweep event

$$u^+ = \Phi y^+, \tag{11}$$

where the mean of  $\Phi$  is 1.84, with minimum and maximum values of 1.60 and 2.14, respectively. These values were used in the Monte Carlo simulations (Section 5) to account for the intensity variation in the burst-sweep events.

The mean aerodynamic lift force is estimated using the results of Mollinger and Nieuwstadt (1996), in which they measured the lift force on 120 and 218  $\mu\text{m}$  diameter microparticles deposited on a surface in the viscous sublayer. The expression is

$$F_L^+ = (56.9 \pm 1.1)R^{+(1.87 \pm 0.04)}, \tag{12}$$

which is valid for  $0.3 < R^+ < 2$ , where  $F_L^+$  is  $F_L/\rho U_\infty^2$ .

Eqs. (3)–(12) form the basis of the theoretical model. Order of magnitude analysis of Eq. (3) shows that the aerodynamic lift and gravitational moments are negligible compared to the drag and pull-off moments. Therefore, for the size range and microparticle density considered in the present experiments, initial detachment is dictated by a balance between the aerodynamic drag and pull-off force moments. That is,

$$1.74RF_D > aF_{PO}. \tag{13}$$

Model predictions are compared with the experimental values of  $U_{th,50\%}$  in Fig. 5. The 95% confidence-level-estimate limits of the model, indicated by dashed curves in the figure, were determined using the Monte Carlo analysis described in Section 5. The predictions and data were found to agree at the 95% confidence level.

The accurate prediction of the threshold-detachment free-stream velocities requires knowledge of the standard deviation of the asperity heights. In this model, this was achieved using the distributions and their means shown in Figs. 2 and 3. This work also addresses the uncertainty that arises if the distribution of the standard deviation of asperity heights is unknown and an *ad hoc* assumption about the value of the factor  $C$  has to be made. The effect of assuming a constant value for the factor  $C$  is illustrated in Fig. 7. In this figure, several numerical simulations for values of  $C$  ranging from 0.5 to 5% are plotted along with the experimental results. It can be seen that small changes in  $C$  produce relatively much larger changes in the threshold-detachment free-stream velocities.

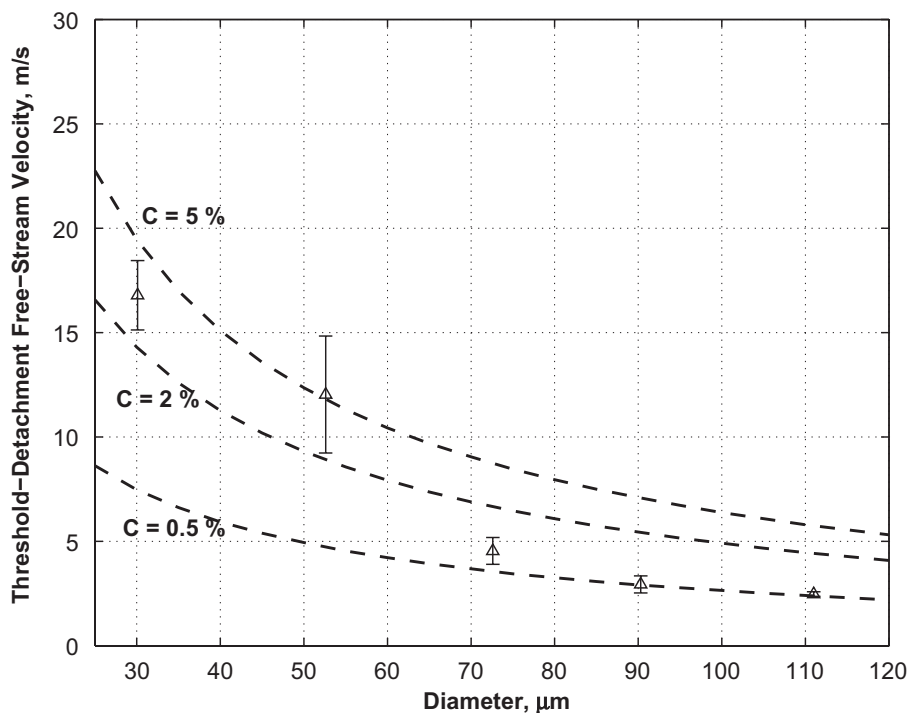


Fig. 7. Different numerical simulation[hs] showing the  $U_{th,50\%}$  for an order-of-magnitude range of the factor  $C$ .

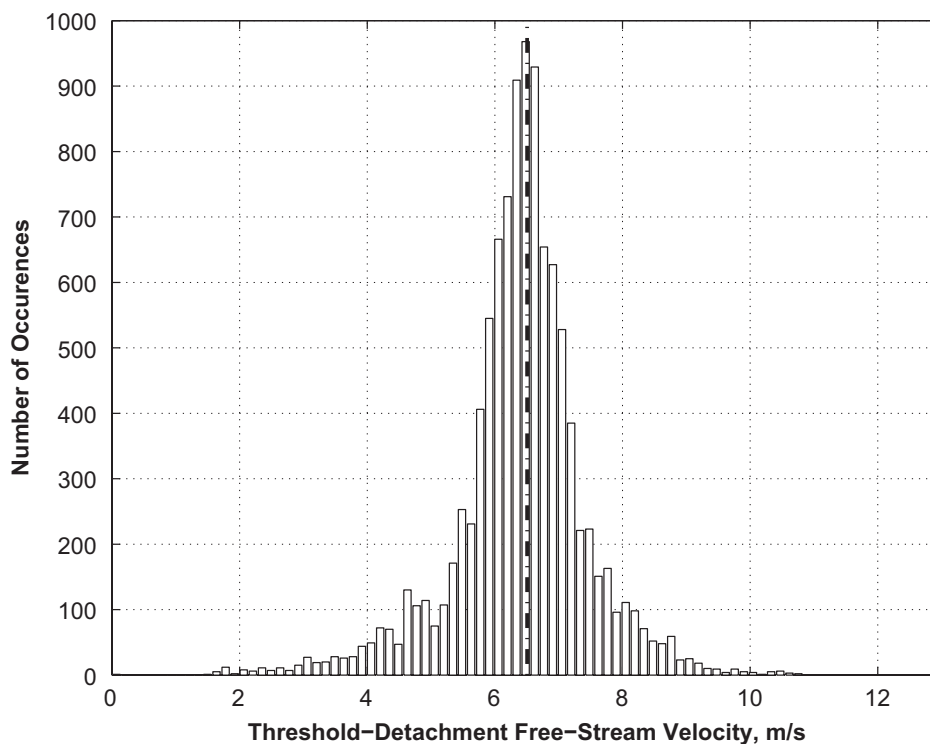


Fig. 8. 10 000 Monte Carlo simulations for the  $U_{th,50\%}$  for a nominal diameter of  $72.6\ \mu\text{m}$ .

## 5. Monte Carlo simulations

Although all the experiments were conducted for the same material combination under controlled conditions as possible, such as relative humidity and mean temporal flow acceleration, several factors related to the *local* environment of each *individual* microparticle could not be controlled directly. These included the inherent variation in local surface roughness at the microparticle/surface interface, the specific microparticle diameter, the variation of physical properties at the interface from their bulk-material values, and the intensity of burst-sweep events in the viscous sublayer. To quantify the effects of these variations on the  $U_{th,50\%}$ , a Monte Carlo analysis comprising of 10 000 simulations was conducted to estimate the theoretical range of the  $U_{th,50\%}$ .

The following factors, as specified by their means and standard deviations (assumed to be normally distributed), were examined:  $\gamma$  ( $0.4\ \text{J/m}^2$ ,  $0.02\ \text{J/m}^2$ );  $v_p$  ( $0.22$ ,  $0.011$ );  $v_s$  ( $0.22$ ,  $0.011$ );  $E_p$  ( $69\ \text{GN/m}^2$ ,  $3.45\ \text{GN/m}^2$ );  $E_s$  ( $69\ \text{GN/m}^2$ ,  $3.45\ \text{GN/m}^2$ );  $\rho_p$  ( $2470\ \text{kg/m}^3$ ,  $123.5\ \text{kg/m}^3$ );  $\phi$  ( $1.84$ ,  $0.135$ ). A standard deviation of 5% in the mean was assumed for all the factors except for  $d$ , for which manufacturer data were used, and for  $\phi$ , where the results of Soltani and Ahmadi (1995) were used. The factor  $\sigma$  was varied according to the mean and distribution shown in Fig. 2 for each microparticle diameter.

Distributions of the possible outcomes of the  $U_{th,50\%}$  were obtained for the five nominal diameters studied. The histogram (constructed according to Williams, 1950) for the  $72.6\ \mu\text{m}$  diameter is shown in Fig. 8. Other diameters showed similar behavior. The results show that the estimated  $U_{th,50\%}$  values follow a normal distribution. The upper and lower uncertainty limits of the model, estimated at 95% confidence, are presented as dashed curves in Fig. 5. These limits were obtained from this Monte Carlo analysis. The average standard deviation of the estimated  $U_{th,50\%}$  values was found to be approximately 25% of their mean values for the five diameters investigated.

## 6. Sensitivity analysis

The sensitivity of the threshold-detachment free-stream velocity,  $U_{th,50\%}$ , to the variables present in the model was assessed. Brach, Li, and Dunn (2000) performed a similar study on microparticle impact and surface capture. In the present study, the following factors were considered: the microparticle diameter,  $d$ , the surface energy of adhesion,  $\gamma$ ,

Table 1  
Full-factorial layout used in the sensitivity analysis

Factors					Response: $U_{th}$
$d$	$\gamma$	$\sigma$	$\Phi$	$K$	
–	–	–	–	–	6.97
+	–	–	–	–	6.36
–	+	–	–	–	7.32
+	+	–	–	–	6.68
–	–	+	–	–	6.81
⋮	⋮	⋮	⋮	⋮	⋮
+	+	–	+	+	6.22
–	–	+	+	+	6.33
+	–	+	+	+	5.77
–	+	+	+	+	6.65
+	+	+	+	+	6.06

the intensity of the burst-sweep event,  $\Phi$ , the standard deviation of asperity heights,  $\sigma$ , and the Hertzian stiffness,  $K$ . It should be noted that although the factor  $C$  significantly affects detachment, it is considered a variable in this model that is dependent on  $\sigma$  and the contact radius,  $a$ , where  $a$  is determined from  $\gamma$ ,  $R$ , and  $K$ .

Sensitivity is determined by examining the effects of the above factors on the response ( $U_{th,50\%}$ ) using the design-of-experiments (DOE) method with a full-factorial design layout (Montgomery, 2004). The above factors were varied by  $\pm 5\%$  and their effects on the  $U_{th,50\%}$  were determined using the revised model.

Table 1 shows the first and last five rows of the factor-level combinations for a  $2^5$  factorial design, where the power 5 represents the number of factors. The (+/–) signs represent the corresponding (high/low) levels of each factor value, which are  $\pm 5\%$  of the nominal values:  $\gamma$  ( $0.4 \text{ J/m}^2$ ),  $d$  ( $72.6 \mu\text{m}$ ),  $\Phi$  (1.84),  $\sigma$  ( $10.27 \text{ \AA}$ ),  $K$  ( $48.3 \text{ GN/m}^2$ ). Data collected according to such a scheme allow the efficient estimation of the relative importance of the factors on controlling the response variable,  $U_{th,50\%}$ .

The main effect of the  $j$ th factor or interaction,  $ME_j$ , is calculated as

$$ME_j = \frac{1}{2^4} \sum_{i=1}^{2^5} \pm U_{th,i} \tag{14}$$

The  $\pm$  signs in Eq. (14) are those corresponding to the appropriate column(s) in Table 1 for each single effect,  $D$ ,  $\gamma$ ,  $\sigma$ ,  $\phi$ , and  $K$  and their interactions. For example, the main effect of the factor  $d$  is  $ME_d = (-6.97 + 6.36 - 7.32 + \dots - 6.65 + 6.06)/16 = -60\%$ . The main effect of the interaction  $d\gamma$  is  $ME_{d\gamma} = (6.97 - 6.36 - 7.32 + \dots - 6.65 + 6.06)/16 = -2\%$  (Guttman, Wilks, & Hunter, 1982).

If the controlled variations of any factor produces no significant effect on the  $U_{th,50\%}$ , the main effect of that factor tends collectively to behave as a small random error. On the other hand, if a factor's variations affect the  $U_{th,50\%}$  significantly, its main effect will stand out from the others. Consequently, the significance of the factors and their interactions can be determined by plotting the main effects and interactions of the factors using a normal-probability axis. Using this approach, insignificant effects exhibit normally distributed random behavior, and, hence, they fall near a straight line on the normal-probability axis. The points that fall away from the line indicate significant factors and interactions. The relative distance from the line indicates the relative significance of the factor or interaction.

The results of the sensitivity analysis are shown in Fig. 9. They indicate that the factors affect the response in the following order and directions:  $d$  ( $-60\%$ ),  $\Phi$  ( $-38\%$ ),  $\gamma$  ( $32\%$ ),  $\sigma$  ( $-17\%$ ), and  $K$  ( $-8\%$ ). Negative signs indicate inverse relationships and positive signs direct relationships. Some second-order interactions also play a lesser role but are comparable with the sensitivity of  $K$ , mainly  $d\gamma$  ( $-2\%$ ) and  $d\phi$  ( $2\%$ ). All other higher-order interactions are negligible.

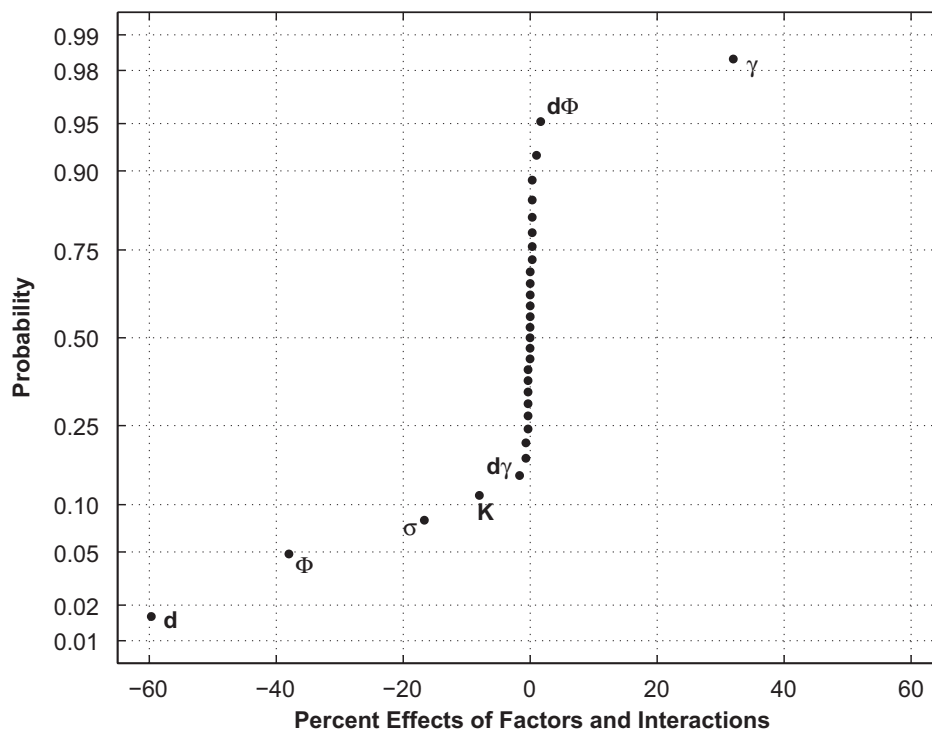


Fig. 9. Design-of-experiment results showing the relative significance of the various factors and interactions examined.

## 7. Summary and conclusions

A new model that accounts for the dependence of the rough-surface pull-off force on the contact radius, as obtained by surface scanning, was presented. This dependence results from the microparticle-surface interface effectively becoming “smoother” as the contact radius becomes smaller. This behavior was observed for contact radii up to  $1\ \mu\text{m}$ . Its effects are more noticeable as the microparticle size decreases. The experimental data were found to agree with the model predictions at the 95% confidence level. The uncertainty in the  $U_{\text{th},50\%}$  resulting from inherent variations in model variables was estimated using a Monte Carlo analysis and found to be approximately 25% of the mean value. A sensitivity analysis was performed on the model and the effects of five different factors on the response were quantified. The input factors affected the  $U_{\text{th},50\%}$  in the following decreasing order: the microparticle diameter, the intensity of the burst-sweep event, the surface energy of adhesion, the standard deviation of asperity heights, and, lastly, the combined stiffness. The results collectively show that an accurate estimate of surface roughness is critical in predicting the threshold-detachment free-stream velocity of a microparticle from a surface.

## Acknowledgments

Research described in this article was supported by Philip Morris USA Inc. and Philip Morris International.

## References

- Braaten, D. A., Paw, U. K. T., & Shaw, R. H. (1990). Particle resuspension in a turbulent boundary layer—observed and modelled. *Journal of Aerosol Science*, 21, 613–628.
- Braaten, D. A., Shaw, R. H., & Paw, U. K. T. (1993). Boundary-layer flow structures associated with particle reentrainment. *Boundary-layer Meteorology*, 65, 255–272.
- Brach, R. M., Li, X., & Dunn, P. F. (2000). Parameter sensitivity in microsphere impact and capture. *Aerosol Science and Technology*, 32, 559–568.
- Cabrejos, F. J., & Klinzing, G. E. (1992). Incipient motion of solid particles in horizontal pneumatic conveying. *Powder Technology*, 72, 51–61.
- Cheng, W., Brach, R. M., & Dunn, P. F. (2002). Surface roughness effects on microparticle adhesion. *Journal of Adhesion*, 78, 929–965.
- Cleaver, J. W., & Yates, B. (1973). Mechanism of detachment of colloidal particles from a flat substrate in a turbulent flow. *Journal of Colloid Interface Science*, 44, 464–474.

- Derjaguin, B. V., Muller, V. M., & Toporov, Y. P. (1975). Effect of contact deformation on the adhesion of particles. *Journal of Colloid and Interface Science*, 53, 314–326.
- Friedlander, S. K. (1977). *Smoke, dust and haze*. New York: Wiley.
- Hontanon, E., de los Reyes, A., & Capitao, J. A. (2000). The CAESAR code for aerosol resuspension in turbulent pipe flows. Assessment against the storm experiments. *Journal of Aerosol Science*, 31, 1061–1076.
- Ibrahim, A. H. (2004). *Microparticle detachment from surfaces by fluid flow*. Ph.D. dissertation, University of Notre Dame.
- Ibrahim, A. H., & Dunn, P. F. (2006). Effects of temporal flow acceleration on the detachment of microparticles from surfaces. *Journal of Aerosol Science*, 37, 1258–1266.
- Ibrahim, A. H., Dunn, P. F., & Brach, R. M. (2003a). Microparticle detachment from surfaces exposed to turbulent air flow: Controlled experiments and modeling. *Journal of Aerosol Science*, 34, 765–782.
- Ibrahim, A. H., Dunn, P. F., & Brach, R. M. (2003b). Microparticle detachment from surfaces exposed to turbulent air flow: Effects of flow and particle deposition characteristics. *Journal of Aerosol Science*, 35, 805–821.
- Ibrahim, A. H., Dunn, P. F., & Brach, R. M. (2004). Microparticle detachment from surfaces exposed to turbulent air flow: Microparticle motion after detachment. *Journal of Aerosol Science*, 35, 1189–1204.
- Guttman, I., Wilks, S., & Hunter, J. (1982). *Introductory engineering statistics*. (3rd ed), New York: Wiley.
- Johnson, K. L., & Greenwood, J. A. (1997). An adhesion map for the contact of elastic spheres. *Journal of Colloid and Interface Science*, 192, 326–333.
- Johnson, K. L., Kendall, K., & Roberts, A. D. (1971). Surface energy and the contact of elastic solids. *Proceedings of the Royal Society of London, Series A*, 324, 301–313.
- Kurose, R., & Komori, S. (1999). Drag and lift forces on a rotating sphere in a linear shear flow. *Journal of Fluid Mechanics*, 384, 183–206.
- Mollinger, A. M. (1995). *Particle entrainment—measurements of the fluctuating lift force*. Ph.D. thesis, Technical University Delft.
- Mollinger, A. M., & Nieuwstadt, F. T. M. (1996). Measurements of the lift force on a particle fixed to the wall in the viscous sublayer of a fully developed turbulent boundary layer. *Journal of Fluid Mechanics*, 316, 285–306.
- Montgomery, D. C. (2004). *Design and analysis of experiments*. New York: Wiley.
- Nicholson, K. W. (1988). A review of particle resuspension. *Atmospheric Environment*, 22, 2639–2651.
- Ockendon, J. R., & Evans, G. A. (1972). The drag on a sphere in low Reynolds number flow. *Journal of Aerosol Science*, 3, 237–242.
- O'Neill, M. E. (1968). A sphere in contact with a plane wall in a slow linear shear flow. *Chemical Engineering Science*, 23, 1293–1298.
- Phares, D. J., Smedley, G. T., & Flagan, R. C. (2000). Effect of particle size and material properties on aerodynamic resuspension from surfaces. *Journal of Aerosol Science*, 31, 1335–1354.
- Podczek, F., Newton, J. M., & James, M. B. (1997). Variations in the adhesion force between a drug and carrier particles as a result of changes in the relative humidity of the air. *International Journal of Pharmaceutics*, 149, 151–160.
- Quon, R. A., Ulman, A., & Vanderlick, T. K. (2000). Impact of humidity on adhesion between rough surfaces. *Langmuir*, 16, 8912–8916.
- Sehmel, G. A. (1980). Particle resuspension: A review. *Environment International*, 4, 107–127.
- Soltani, M., & Ahmadi, G. (1994). On particle adhesion and removal mechanisms in turbulent flows. *Journal of Adhesion Science and Technology*, 8, 763–785.
- Soltani, M., & Ahmadi, G. (1995). Direct numerical simulation of particle entrainment in turbulent channel flow. *Physics of Fluids*, 7, 647–657.
- Taheri, M., & Bragg, G. M. (1992). A study of particle resuspension in a turbulent flow using a Pitot probe. *Journal of Adhesion Science and Technology*, 16, 15–20.
- Tsai, C. J., Pui, D. Y. H., & Liu, B. Y. H. (1991). Particle detachment from disk surfaces of computer disk drives. *Journal of Aerosol Science*, 22, 737–746.
- Williams, C. A. (1950). On the choice of the number and width of classes for the Chi-square test of goodness-of-fit. *Journal of American Statistical Association*, 45, 77–88.
- Yiantsios, S. G., & Karabelas, A. J. (1995). Detachment of spherical microparticles adhering on flat surfaces by hydrodynamic forces. *Journal of Colloid and Interface Science*, 176, 74–85.
- Zimon, A. D. (1982). *Adhesion of dust and powders*. (R. K. Johnston, Trans.) New York: Consultants Bureau, (Translated from Russian).
- Ziskind, G. (2006). Particle resuspension from surfaces: Revisited and re-evaluated. *Reviews in Chemical Engineering*, 22, 1–123.
- Ziskind, G., Fichman, M., & Gutfinger, C. (1995). Resuspension of particulates from surfaces to turbulent flows: Review and analysis. *Journal of Aerosol Science*, 26, 613–644.
- Ziskind, G., Fichman, M., & Gutfinger, C. (1997). Adhesion moment model for estimating particle detachment from a surface. *Journal of Aerosol Science*, 28, 623–634.